Precursory transient slip during the 2001 M_w = 8.4 Peru earthquake sequence from continuous GPS

Timothy I. Melbourne
Department of Geological Sciences, Central Washington University, USA

Frank H. Webb
Jet Propulsion Laboratory, California Institute of Technology, USA

Received 22 May 2002; accepted 6 August 2002; published 13 November 2002.

[1] Two-hour position estimates from a continuous GPS station located at Arequipa, Peru, document precursory deformation beginning 18 hours prior to an M_w = 7.6 aftershock of the June 23rd 2001 M_w = 8.4 earthquake. This preseismic signal appears on the north and east components as a slow displacement with an amplitude twice that of the subsequent coseismic. Analysis of three years of 18-hour rate measurement shows this signal to be unprecedented and beyond four standard deviations from the mean rate. The best fitting centroid is directionally consistent with slow slip along the plate interface and suggests the preseismic deformation arises from creep near the aftershock rupture. This implies the Nazca-South American plate interface slipped slowly prior to seismogenic faulting. These observations indicate the M_w = 7.6 earthquake grew out of slow slip along the plate interface and clearly demonstrate the breadth of slip rates accommodated by subduction zone plate interfaces. *INDEX TERMS:* 1206 Geodesy and Gravity: Crustal movements—interplate (8155); 7209 Seismology: Earthquake dynamics and mechanics; 7230 Seismology: Seismicity and seismotectonics; 8123 Tectonophysics: Dynamics, seismotectonics. **Citation:** Melbourne, T. I., and F. H. Webb, Precursory transient slip during the 2001 M_w = 8.4 Peru earthquake sequence from continuous GPS, *Geophys. Res. Lett.*, *29*(21), 2032, doi:10.1029/2002GL015533, 2002.

1. Introduction

[2] The M_w = 8.4 June 23, 2001 Peru earthquake ruptured the Nazca-South American plate interface to become the largest event in the last 30 years. Teleseismic analyses indicate that rupture initiated offshore southern Peru and propagated southeast. The largest asperity, representing slip estimated as high as nine meters, lies nearly 200 km southeast of the nucleation site (Figure 1; [*Dziewonski et al.*, 2001; *Kikuchi and Yamanaka*, 2001]). The mainshock was followed by a vigorous aftershock sequence, including three events with moment magnitudes of M_w = 6.7, 6.5, and on July 7, an M_w = 7.6 event. Mainshock coseismic displacement greater than 50 cm, along with aftershock and rapid postseismic deformation, were recorded on a continuously operating GPS station operated by NASA for the International GPS Service (IGS) located at Arequipa (AREQ), Peru (Figures 2–3).

0094-8276/02/2002GL015533$05.00

[3] The July 7 M_w = 7.6 event was located at 25 km centroid depth, within the primary mainshock asperity [*Kikuchi and Yamanaka*, 2001]. This region lies up-dip of the meta-stable interface region in which rapid creep is inferred to explain postseismic vertical uplift (compared to coseismic subsidence) that dominates the AREQ time series over the months following the mainshock [*Melbourne et al.*, 2002]. Non-seismogenic slip rates are of interest because they provide constraints on the frictional properties of the plate interface at depth, which are complex. Thermal and constitutive models of most subduction zones indicate the plate interface transitions down-dip from purely stick-slip, seismogenic rupture to stable sliding, between which creep can occur but runaway fault rupture cannot self-nucleate [*Dieterich*, 1992; *Marone and Scholz*, 1988]. Only a few slow-faulting events have thus far been detected, and any new observations of slow slip, particularly precursory slow slip, are of interest. Analysis of anomalous, preseismic deformation prior to the M_w = 7.6 aftershock is the subject of this paper.

2. Data Analysis and Transient Slip

[4] AREQ is the only publicly available continuously operating GPS station within the region affected prior to, during and after the mainshock and its aftershocks. Conclusions based on AREQ could be tested using nearby concurrent GPS data taken to monitor El Misti volcano, which were not made available upon request for the purpose of this study. AREQ is operated by NASA/JPL as part of the IGS http://igscb.jpl.nasa. gov/network/site/areq.html). It is a typical geodetic quality IGS station, consisting of a dual frequency receiver and choke ring antenna attached to a stable foundation, in this case a concrete pillar set several meters into the ground. Installed in 1994, the station has been routinely used as a stable reference point within the global IGS network for reference frame studies and orbit calculations.

[5] The AREQ data were precise point positioned using the GIPSY-OASIS II software [*Zumberge et al.*, 1997] and GPS orbit and clock parameters calculated by JPL and submitted to the IGS. Station positions were estimated as stochastic processes with white noise resets every 2 hours using 24-hour data arcs. By applying stochastic resets to the coordinates only, the geometric strength of the 24-hour data arc for estimating carrier phase biases and atmospheric delays is retained. Station position estimates are thus obtained at a higher rate without significant systematic

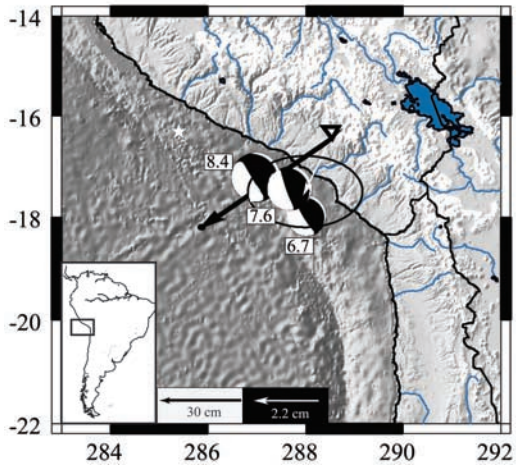

Figure 1. Measured GPS offsets during the 06/23/01 M_w = 8.4 Peru mainshock and aftershocks. Solid black vector shows coseismic displacements due to the mainshock, white vector denotes measured preseismic offset prior to the July 7 M_w = 7.6 aftershock. Error ellipses are 2σ. White star shows National Earthquake Information Center rupture nucleation site. Triangle denotes position of the IGS GPS station located at Arequipa, Peru.

artifacts associated with the higher frequency error sources. Additional resets were forced at reported mainshock and aftershock times.

[6] Modeling station positions as white noise, although noisier than a random walk, is the most conservative approach to identifying transient deformation. This stems from the fact that subsequent position estimates remain uncorrelated in time, which is not the case with random walks. Moreover, the white-noise approach side steps the need to establish an a priori rate of random walk process noise which neither suppresses a true signal nor introduces erroneous deformation artifacts, as discussed in *Larson et al.* [2001]. Ocean tide loading of the crust was accounted for using modelcoefficients based on *Scherneck* [1991], which reduce periodicities due to tidal harmonics. The north-south and east-west amplitudes of the semi-diurnal M_2, S_2 and K_2 coefficients average less than 2 mm, with the largest amplitude being 2.8 mm, less than 10% of the observed preseismic deformation.

[7] The AREQ time series show deformation over timescales ranging from years to seconds (Figures 2–3). The χ^2-fit of two years of deformation prior to the mainshock indicate a northeast directed interseismic velocity of 2.1 ± 0.3 cm/year at azimuth N53W. Inspection of position estimates prior to the M_w = 8.4 mainshock show no credible evidence of short-term precursory deformation, although a change in interseismic deformation rate beginning one month prior to the event has been reported in *Ruegg et al.* [2001]. The mainshock and larger aftershocks appear as discontinuities in the time series (Figure 3) and are followed by rapid postseismic deformation at rates of cm per week, similar in style to that seen following large thrust events offshore Kamchatka, western Mexico, and Japan [*Bürgmann et al.*, 2001; *Melbourne et al.*, 2002].

[8] Roughly 18 hours prior to the July 7 M_w = 7.6 aftershock, the north and east components of position depart from the postseismic trend by nearly three centimeters, well in excess of the two and four mm of scatter in the time series over 11 days prior to July 7 (Figure 3). On the north component, where the signal is strongest, calculation of rates of offset based on 18 hours of AREQ data starting two

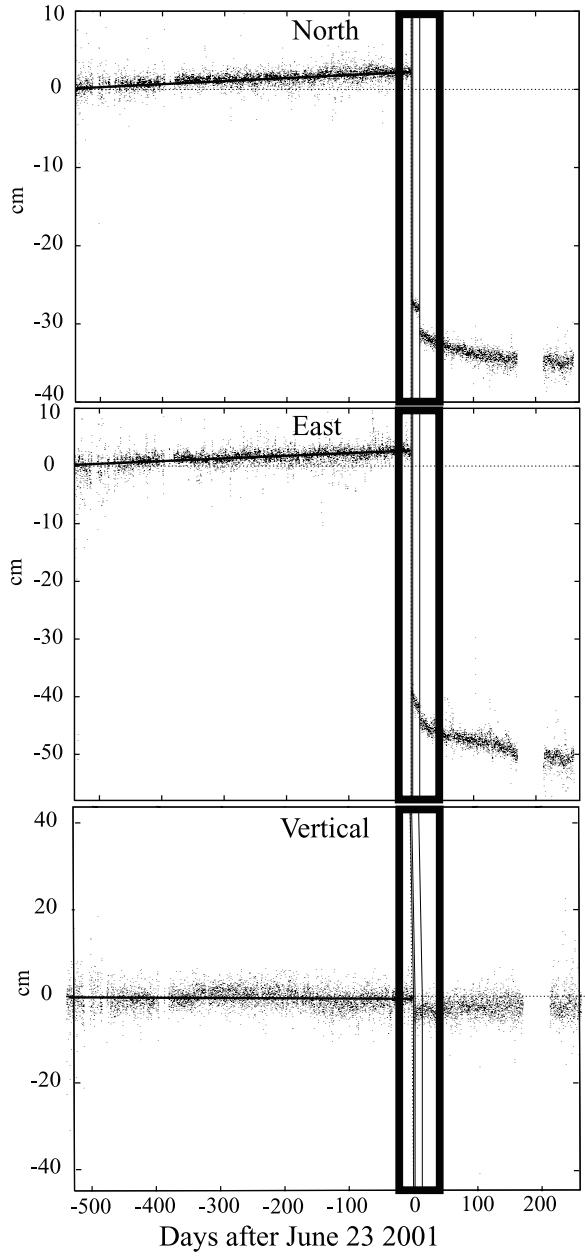

Figure 2. Two hour position solutions show interseismic, coseismic and postseismic deformation recorded at Arequipa between two years prior to and 9 months after the June 23 2001 M_w = 8.4 event. Heavy black squares denote zoom area shown in Figure 3. Thin solid black lines show times of seismogenic rupture reported by the Global Seismic Network. χ^2-fit of interseismic strain accumulation rates in the north, east and vertical components measure 1.2 ± .02, 1.6 ± .02, and −0.26 ± .04 cm/year, respectively, and are shown with solid line.

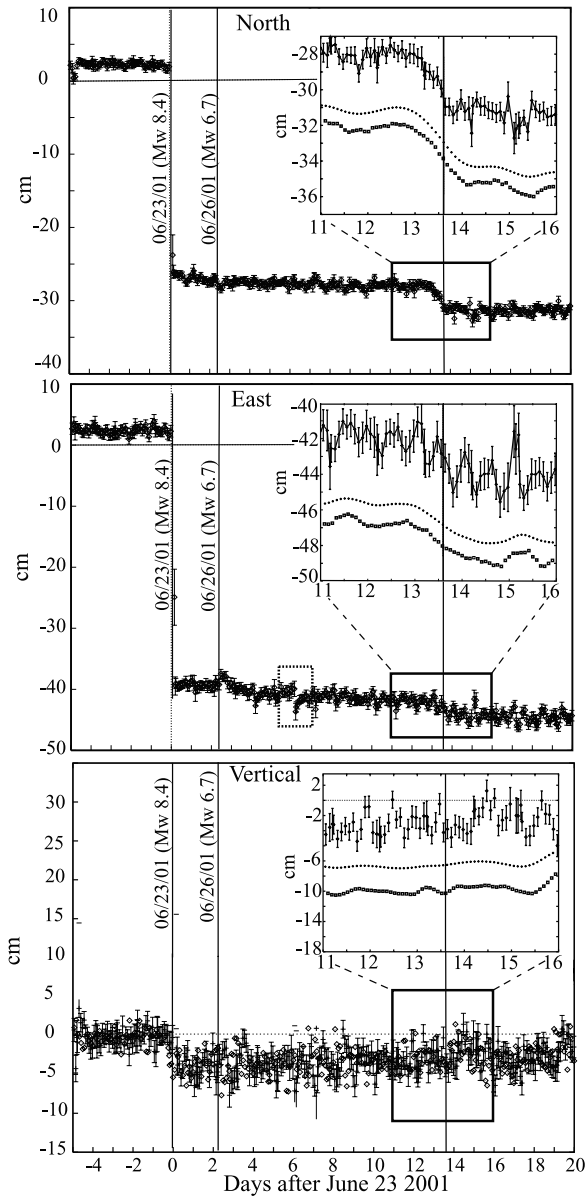

Figure 3. Coseismic deformation recorded at AREQ from the mainshock and two major aftershocks. Vertical lines denote times of major aftershocks. Preseismic deformation prior to the July 7 Mw = 7.6 aftershock is visible on the north and east components. Zoom of the five-day period around the July 7 aftershock (Inset) shows that on the north component, where signal scatter is lowest and preseismic deformation signal is largest, deformation starts ~18 hours prior to the aftershock. Inset crosses are computed with an acausal n = 3 symmetric smoothing window, squares a causal, single-pass Butterworth filter with a 12- hour corner. Both filtered times series show ~2 cm of southerly and ~1 cm of westerly preseismic motion. No deformation is visible on the vertical component. On the east component, the significant <3 cm offset on June 29th, six days after the mainshock, shown inside the dashed box, does not correspond to any teleseismically reported earthquake. Its total duration is less than 6 hours, during which time the position returns to the mean value for the two days prior to and after the jump.

years prior to and ending 9 months after July, 2001 show no other instances of comparable deformation rates except at the time of the mainshock. With nearly 9000 possible 18-hour windows, the precursory rate has an amplitude more than four standard deviations from the mean 18-hour rate. This precludes it being an artifact of random error.

[9] On the north component of motion, the preseismic signal manifests itself clearly as 2.0 ± 0.5 cm of southerly offset, while on the east component the offset is evident but obscured by a near-24-hour beating likely due to multi-pathing. To quantify the easterly offset, we use two filtering schemes, a symmetric but acausal, three-point half width smoothing window (crosses, Figure 3 inset) and a causal, one pass 12-hour corner Butterworth filter (squares). Applied to the north, filtering replicates that readily visible without filtering. In the east, it brings out −1 ± 0.5 cm of preseismic offset that is simultaneous with the north. The uncertainties on this estimate are nearly 50% of the signal, but the sense of preseismic motion is extension at azimuth of N150E, consistent with reverse faulting along the plate interface.

[10] It is well known that zenith tropospheric delay estimates are correlated with estimates of the vertical position and station clocks (e.g., *Segall and Davis* [1997]). If precursory horizontal motion were due to some unknown atmospheric signal, it should be most noticeable in these parameters. However, the station clocks show no anomalous behavior in either amplitude or rate of change during the time around July 7. Moreover, the vertical position, which would be offset well above the noise given the horizontal signal, is not, also suggesting the precursor is not an artifact of unmodeled tropospheric noise. Estimation of tropospheric gradients also fails to remove the precursory signal. Correlation between the north and east positions are not anomalous in either amplitude or rate of change around July 7, precluding satellite coverage, geometry, or data processing as the source of the signal. The signal to noise ratio of the AREQ GPS receiver itself is not deviant during this period. Tests of satellite cut off angle ranging from 0 to 45° at AREQ show that dependency of horizontal positions on the cut off angle are less than 5 mm, well below the observed signal. Finally, station positions do not rebound from the combined pre- and coseismic July 7 offsets, most of which comes from the preseismic signal, over the following months as expected for multi-pathing. Together, the fact that the signal is unprecedented, our inability to ascribe it to non-tectonic processes, that it is a permanent shift consistent with slow interface slip, and that it is both preceded and succeeded over days by slow and seismogenic slip, we conclude the preseismic deformation is caused by slow faulting prior to the M_w = 7.6 aftershock.

[11] A key issue regarding this precursor is to understand the spatial relationship between the precursory and seismogenic aftershock slip. For instance, if the two are not proximal, then the observed deformation documents an isolated, transient, 'slow earthquake' lasting hours, faster but similar in nature to that reported in subduction zones offshore Japan, Alaska, Mexico and Cascadia [*Dragert et al.*, 2001; *Freymueller et al.*, 2001; *Hirose et al.*, 1999; *Kawasaki et al.*, 1995; *Lowry et al.*, 2001]. If they are proximal, the deformation documents precursory slip prior to seismogenic rupture.

[12] With data from only one station, it is impossible to pinpoint the location of preseismic slip. However, because we know the geometry and convergence direction of the plate interface, we can make a coarse estimation of the average azimuth of preseismic slip relative to AREQ. A fundamental caveat of course is that there exist an infinite number of heterogeneous slip distributions that could produce the identical offset at AREQ. The down dip location of preseismic slip cannot be constrained using the AREQ data due to the high level of noise in the vertical component. By assuming the faulting occurred along the Nazca-South American plate interface, whose location and dip are based on independent data and held fixed [*Tavera and Buforn*, 1998] and by fixing the preseismic focal mechanism to the rake predicted by Nuvel-1 (convergence azimuth of 75°), we then allow the thrust centroid to vary along-strike and solve for the position that best replicates the observed preseismic offsets.

[13] For the mainshock, the coseismic vector yields a best-fitting centroid that overlies the CMT location in map view (Figure 1). For the preseismic, the best-fitting centroid lies about 10° southeast azimuth from the aftershock CMT location implies, to the extent that one station can constrain it, the preseismic and M_w = 7.6 coseismic slip are mechanistically related. This conclusion is also supported by the fact that the preseismic creep is terminated by the aftershock, which would be coincidental if the two were mechanistically unrelated.

[14] Modeling indicates that the preseismic moment is roughly a factor of two greater than the coseismic aftershock moment (M_w = 7.8), and this is not strongly dependent on the down-dip location of the precursory slip. The presence of intermediate-rate faulting over tens of minutes is not constrained by these data but could be detected on global seismic network spectra. Teleseismically, the aftershock appears normal, and lacks any visible slow onset or rupture [*Bilek and Ruff*, 2002]. Thus, no inferences about creep acceleration can be made, although the GPS data do clearly illustrate a wide range of slip rates that likely reflects the interplay of variable constitutive properties.

[15] **Acknowledgments.** The research described in this paper was supported by a National Science Foundation grant EAR-0003483 to Melbourne and carried out at Central Washington University and the Jet Propulsion Laboratory, California Institute of Technology, under a contract with the National Aeronautics and Space Administration.

References

Bilek, S. L., and L. J. Ruff, Analysis of the 06/23/01 Mw = 8.4 Peru Underthrusting Earthquake and its Aftershocks, *Submitted to Geophysical Research Letters*, 2002.

Bürgmann, R., M. G. Kogan, V. E. Levin, C. H. Scholz, R. W. King, and G. M. Steblov, Rapid aseismic moment release following the 5 December 1997 Kronotsky, Kamchatka, earthquake, *Geophysical Research Letters*, *28*(7), 1331–1334, 2001.

Dieterich, J. H., Earthquake nucleation on faults with rate- and state-dependent strength, in *International symposium on Earthquake source physics and earthquake precursors*, edited by T. Mikumo, K. Aki, M. Ohnaka, L. J. Ruff, and P. K. P. Spudich, pp. 115–134, Elsevier, 1992.

Dragert, H., K. Wang, and T. S. James, A silent slip event on the deeper Cascadia subduction interface, *Science*, *292*(5521), 1525–1528, 2001.

Dziewonski, A. M., G. Ekstrom, and M. P. Salganik, Harvard Centroid Moment Tensors, 2001.

Freymueller, J., C. Zweck, H. Fletcher, S. Areinsdottier, S. C. Cohen, and M. Wyss, *Eos Trans. Am. Geophys. Union*, *82*(47), (Fall Meet. Suppl., Abstract G22D-11), 2001.

Hirose, H., K. Hirahara, F. Kimata, N. Fujii, and S. i. Miyazaki, A slow thrust slip event following the two 1996 Hyuganada earthquakes beneath the Bungo Channel Southwest Japan, *Geophysical Research Letters*, *26*(21), 3237–3240, 1999.

Kawasaki, I., Y. Asai, Y. Tamura, T. Sagiya, N. Mikami, Y. Okada, M. Sakata, and M. Kasahara, The 1992 Sanriku-Oki, Japan, ultra-slow earthquake, *Journal of Physics of the Earth*, *43*(2), 105–116, 1995.

Kikuchi, M., and Y. Yamanaka, Earthquake Information Center Seismological note no. 105, Earthquake Information Center, Earthquake Research Institute, University of Tokyo, 2001.

Larson, K. M., P. Cervelli, M. Lisowski, A. Miklius, P. Segall, and S. Owen, Volcano monitoring using the Global Positioning System; filtering strategies, *Journal of Geophysical Research B, Solid Earth and Planets*, *106*(9), 19,453–19,464, 2001.

Lowry, A. R., K. M. Larson, V. Kostoglodov, and R. Bilham, Transient fault slip in Guerrero, southern Mexico, *Geophysical Research Letters*, *28*(19), 3753–3756, 2001.

Marone, C., and C. H. Scholz, The depth of seismic faulting and the upper transition from stable to unstable slip regimes, *Geophysical Research Letters*, *15*(6), 621–624, 1988.

Melbourne, T., F. H. Webb, J. Stock, and C. Reigber, Rapid postseismic transients in subduction zone earthquakes from continuous GPS, *Journal of Geophysical Research*, in press, 2002, available at www.geology.cwu.edu/facstaff/tim, 2002.

Ruegg, J. C., M. Olcay, and D. Lazo, Co-, Post- and Pre(?)-seismic Displacements Associated with the Mw 8.4 Southern Peru Earthquake of 23 June 2001 from Continuous GPS Measurements, *Seismological Research Letters*, *72*(6), 673–678, 2001.

Scherneck, H. G., A parametrized solid Earth tide model and ocean tide loading effects for global geodetic baseline measurements, *Geophysical Journal International*, *106*(3), 677–694, 1991.

Segall, P., and J. L. Davis, GPS applications for geodynamics and earthquake studies, *Annual Review of Earth and Planetary Sciences*, *25*, 301–336, 1997.

Tavera, H., and E. Buforn, Seismicity and seismotectonics of Peru, in *23rd general assembly of the European Geophysical Society*, edited by Anonymous, pp. 160, European Geophysical Society, 1998.

Zumberge, J. F., M. B. Heflin, D. C. Jefferson, M. M. Watkins, and F. H. Webb, Precise point positioning for the efficient and robust analysis of GPS data from large networks, *Journal of Geophysical Research, B, Solid Earth and Planets*, *102*(3), 5005–5017, 1997.

T. I. Melbourne, Department of Geological Sciences, Central Washington University, Ellensburg, WA 98926, USA. (tim@geophysics.cwu.edu)

F. H. Webb, Jet Propulsion Laboratory, California Institute of Technology, 4800 Oak Grove Dr., Pasadena, CA 91109, USA. (fhw@cobra.jpl.nasa.gov.)